Published in final edited form as:

Dev Dyn. 2010 January ; 239(1): 237–245. doi:10.1002/dvdy.22101.

Genetic Interaction Between *Lrp6* and *Wnt5a* During Mouse Development

Emma Andersson[1,†,‡], **Lenka Bryjova**[1,2,†], **Kristin Biris**[3], **Terry P. Yamaguchi**[3], **Ernest Arenas**[1,*], **Vítězslav Bryja**[1,2,*]

[1]Molecular Neurobiology, Department of Medical Biochemistry & Biophysics, Karolinska Institutet, Stockholm, Sweden [2]Institute of Experimental Biology, Faculty of Science, Masaryk University & Department of Cytokinetics, Institute of Biophysics, Academy of Sciences of the Czech Republic, Brno, Czech Republic [3]Cancer and Developmental Biology Laboratory, Center for Cancer Research, National Cancer Institute-Frederick, NIH Frederick, Maryland

Abstract

Lrp6 is generally described as a receptor required for signal transduction in the Wnt/β-catenin pathway. *Wnt5a*, however, is a Wnt ligand that usually does not activate Wnt/β-catenin but rather activates noncanonical Wnt signaling. We have previously shown that *Lrp6* can inhibit noncanonical *Wnt5a/Wnt11* signaling and that *Lrp5/6* loss-of-function produces noncanonical gain-of function defects, which can be rescued by loss of *Wnt5a*. Here, we describe other phenotypes found in *Wnt5a/Lrp6* compound mutant mice, including a worsening of individual *Wnt5a* or *Lrp6* loss of function phenotypes. *Lrp6* haploinsufficiency in a *Wnt5a−/−* background caused spina bifida and exacerbated posterior truncation. *Wnt5a−/−Lrp6−/−* embryos displayed presomitic mesoderm morphogenesis, somitogenesis, and neurogenesis defects, which are much more severe than in either of the single mutants. Interestingly these results reveal a further level of complexity in processes in which *Wnt5a* and LRP6 cooperate, or oppose each other, during mouse development.

Keywords

Wnt5a; *Lrp6*; somitogenesis; development

INTRODUCTION

Wnts are a family of secreted glycoproteins that regulate several processes during embryonic development including proliferation, migration, cell polarity, and differentiation (Logan and Nusse, 2004; Montcouquiol et al., 2006). Signaling components have been classically divided into canonical and noncanonical pathway components depending on their ability to

*Correspondence to: Vítězslav Bryja, Institute of Experimental Biology, Faculty of Science, Masaryk University, Kotlarska 2, 611 37, Brno, Czech Republic. bryja@sci.muni.cz and Ernest Arenas, Laboratory of Molecular Neurobiology, Department of Medical Biochemistry & Biophysics, Karolinska Institutet, Stockholm, Sweden. Ernest.Arenas@ki.se.

†Drs. Andersson and Bryjova contributed equally to this work.

‡Dr. Andersson's present address is Department of Cell and Molecular Biology, Karolinska Institutet, Stockholm, Sweden.

transform C57MG mammary cells (Wong et al., 1994) and induce axis duplication in *Xenopus* (Sokol et al., 1991). By these standards, and based on their effect (or lack thereof) on β-catenin stabilization, *Wnt5a* has been classified as a noncanonical Wnt (Moon et al., 1993; Wong et al., 1994; Torres et al., 1996), while the low-density lipoprotein-related receptor (Lrp)6 has been classified as a canonical Wnt co-receptor (for review, see He et al., 2004). As such, *Wnt5a* and *Lrp6* were not previously thought to interact. However, recent reports have shown that *Lrp6* can affect typical noncanonical processes, and modulate *Wnt5a*-regulated processes in both *Xenopus* and mouse (Tahinci et al., 2007; Bryja et al., 2009).

We have previously reported the derivation and characterization of mice harboring simultaneous mutations in both *Wnt5a* (Yamaguchi et al., 1999a; Andersson et al., 2008) and *Lrp6* (Pinson et al., 2000; Bryja et al., 2009). Analysis of these compound mutant mice showed that loss of *Wnt5a* rescues exencephaly, a typical planar cell polarity (PCP)/convergent extension (CE) defect, as well as heart defects, otherwise seen in *Lrp6−/−* embryos, while *Wnt5a−/−Lrp6−/−* mutants are severely developmentally delayed (Bryja et al., 2009). These previous results hinted at a dose-dependent interaction between *Wnt5a* and *Lrp6*, but also indicated that Wnt5a and Lrp6 may cooperate in some developmental processes/tissues, while acting in opposing fashions in others (such as PCP/CE).

Here, we describe additional phenotypes that demonstrate a genetic interaction between *Wnt5a* and *Lrp6*, including spina bifida, posterior truncation, presomitic mesoderm morphogenesis, somitogenesis, and neurogenesis defects, all of which confirm the crucial importance of *Lrp6* and *Wnt5a* in the development of these structures. Furthermore, these results reveal further processes in which *Wnt5a* and *Lrp6* cooperate or oppose each other during mouse development.

RESULTS

General Phenotype of *Wnt5a/Lrp6* Compound Mutants

We have previously shown that *Wnt5a+/−Lrp6+/−* animals are born with the expected frequency and do not show any obvious morphological, fertility, or behavioral defects in comparison with parental *Wnt5a* or *Lrp6* heterozygotes. Mating of *Wnt5a+/−Lrp6+/−* mice generated *Wnt5a−/−Lrp6−/−* embryos with the expected frequency at E10.5 (Bryja et al., 2009). All *Wnt5a−/−Lrp6−/−* embryos were severely developmentally delayed at E10.5, and we did not obtain any *Wnt5a−/−Lrp6−/−* embryos at E12.5. A general morphological assessment of all studied genotypes is shown in Figure 1. *Wnt5a−/−Lrp6+/+* and *Wnt5a−/−Lrp6+/−* embryos are indistinguishable at this stage and display a phenotype characterized by limb defects and a shorter anteroposterior (AP) body axis, which can be clearly diagnosed in the tail region (here referred to as "*Wnt5a* phenotype"). In contrast, *Wnt5a+/+Lrp6−/−* embryos are more variable in their phenotype. Typically they display a compound phenotype characterized at this stage by slightly delayed development (embryos are smaller), a less well-defined isthmus, and defects in tail development, often manifesting in the form of a kinked tail (here referred to as "*Lrp6* phenotype"). Exencephaly is observed in approximately 30% of *Lrp6−/−Wnt5a+/+* embryos (yellow arrow in Fig. 1A, and brain section in Fig. 1B). *Wnt5a+/−Lrp6−/−* embryos are usually similar in morphology to *Wnt5a*

+/+Lrp6−/− embryos, but in approximately 40% of *Wnt5a+/−Lrp6−/−* embryos we observed a severe developmental delay and defects in heart morphogenesis (see Fig. 1A, embryo #2 for this phenotype). As we have shown previously (Bryja et al., 2009), the incidence of exencephaly is less than 10% in *Wnt5a+/−Lrp6−/−* embryos. *Wnt5a−/−Lrp6−/−* embryos show a severe, although to some extent variable, phenotype which is characterized by general developmental delay (with a size less than 40% of wild-type littermates) and a lack of embryonic turning (red arrowhead in Fig. 1A). Furthermore, heart morphogenesis is disrupted, and embryos manifest a grossly enlarged pericardium (white arrowhead in Fig. 1A), as well as a tubular, unlooped heart (yellow arrowhead in Fig. 1A). All these phenotypes are highly penetrant and appear in almost 100% of embryos (Fig. 1C).

Later during development at E14.5, *Wnt5a−/−* mice show a complex phenotype characterized by craniofacial malformations, lack of digits in the limbs, shortening of the AP axis, and edema (Fig. 2A; Yamaguchi et al., 1999a; Yang et al., 2009). *Lrp6−/−* embryos at embryonic day (E) 14.5 display a complete penetrance in eye developmental defects, posterior truncation, spina bifida, and in defects in the limbs, which exhibit a reduced number of digits (Fig. 2A; Pinson et al., 2000; Adamska et al., 2005; Zhou et al., 2008) *Wnt5a−/−Lrp6+/−* embryos resemble *Wnt5−/−Lrp6+/+* embryos.

Haploinsufficiency for *Lrp6* did not affect the edema, craniofacial or limb defects seen in *Wnt5a−/−* mice (data not shown and Fig. 2A), but a slight reduction in size was observed in some *Wnt5a−/−Lrp6+/−* mice when compared with littermate *Wnt5a−/−Lrp6+/+* embryos (Fig. 2A). Importantly, *Wnt5a−/−Lrp6+/+* and *Wnt5a−/−Lrp6+/−* embryos were recovered at the expected equal frequencies at E12.5, whereas at E14.5, we obtained fewer *Wnt5a−/−Lrp6+/−* embryos than *Wnt5a−/−Lrp6+/+* embryos, indicating increased mortality of *Wnt5a−/−Lrp6+/−* embryos between E12.5 and E14.5 (Fig. 2B). Haploinsufficiency for *Wnt5a* in the *Lrp6−/ −* background negatively affected embryo survival at both E12.5 and E14.5 (Fig. 2B). The decreased proportion of *Wnt5a+/−Lrp6−/−* embryos, observed as early as E12.5, may reflect the death of the group of *Wnt5a+/−Lrp6−/−* embryos that were severely developmentally delayed, with heart defects, seen at E10.5 (Fig. 1B). *Wnt5a+/−Lrp6−/−* embryos, which survived to E14.5, were often anemic and smaller than *Wnt5a+/+Lrp6−/−* embryos. However, approximately 60% of these embryos showed the same morphology as *Wnt5a+/+Lrp6−/−* embryos (Fig. 2A) and we did not observe any amelioration/aggravation of the eye phenotype, digit number, or spina bifida, which was present with almost 100% penetrance both in *Wnt5a+/−Lrp6−/−* and *Wnt5a+/+Lrp6−/−* embryos.

It has previously been shown that loss of certain Wnt signaling components, such as Dvl2, affects survival in a gender-specific manner, such that more females are born (Hamblet et al., 2002), whereas loss of Wnt4 revealed its role in gender development (Vainio et al., 1999). We have previously shown that *Wnt5a* treatment leads to the phosphorylation and mobility-shift of Dvl2 (Schulte et al., 2005; Bryja et al., 2007b), whereas other studies have shown that Dvl2 is involved in the phosphorylation of *Lrp6* (Bilic et al., 2007). Because many of the phenotypes observed in the *Wnt5a* and *Lrp6* single or compound mutant mice, such as heart outflow tract defects or exencephaly (Schleiffarth et al., 2007; Bryja et al., 2009), are reminiscent of Dvl2 mutant mouse phenotypes (Hamblet et al., 2002), we asked whether the

proportion of male and female mice was affected by a genetic interaction between *Wnt5a* and *Lrp6.* Gender-specific polymerase chain reaction (PCR), using SMCX-1 and SMC4-1 primers, revealed that 53% of *Wnt5a−/−Lrp6+/+* embryos recovered between E12.5 and E14.5 were female, whereas 63% of *Wnt5a−/−Lrp6+/−* embryos were female (Fig. 2C). Conversely, 67% of recovered *Wnt5a+/+Lrp6−/−* embryos at E12.5 to E14.5 were female, which was rescued to 50% in *Wnt5a+/−Lrp6−/−* mice. Although these differences were not statistically significant, the tendency for loss of *Lrp6* to bias toward a female fate and the opposing effect of *Wnt5a* and *Lrp6* on gender survival, indicate yet another level at which *Wnt5a* and *Lrp6* may oppose one another.

Lrp6 Haploinsufficiency Aggravates Anteroposterior Defects Seen in *Wnt5a−/−* Mice

We next analyzed possible reasons for the decreased survival of *Wnt5a−/−Lrp6+/−* embryos between E12.5 and E14.5, and compared defects between *Wnt5a−/−Lrp6+/−* and *Wnt5a−/−Lrp6+/+* embryos at E12.5. *Wnt5a* is required for the outgrowth of several structures including the snout, ears, genitals, and limbs, and loss of *Wnt5a* also causes AP elongation defects (Yamaguchi et al., 1999a; Andersson et al., 2008). At E12.5, 80% of *Wnt5a−/−* embryos display moderate AP defects (Fig. 3A, subpanel a, a') with symmetrical hindlimbs (yellow arrowheads) and a rudimentary tail (black arrowhead). The remaining 20% display slightly more severe defects, with asymmetrical hindlimbs (Fig. 3A, subpanel b, b′). Interestingly ablation of a single allele of *Lrp6* on a *Wnt5a−/−* background greatly affected the severity of these caudal defects, and thus no *Wnt5a−/−Lrp6+/−* embryos displayed mild defects. Instead, the majority of *Wnt5a−/−Lrp6+/−* embryos (60%) displayed intermediate defects (Fig. 3A, subpanel 2, 2′), and the remaining *Wnt5a−/−Lrp6+/−* embryos displayed a much more severely affected caudal region, with rudimentary asymmetrical hindlimbs (30%, Fig. 3A, subpanel c, c′) or a complete lack of caudal structures such as a tail rudiment or hindlimbs (10%, Fig. 3A, subpanel d, d′).

We have previously shown that 30% of *Lrp6−/−* mice exhibit exencephaly, a neural tube closure defect in the anterior neural tube, which is dose-dependently rescued by loss of *Wnt5a* (Fig. 1B) (Bryja et al., 2009; Castelo-Branco et al., 2009). Another neural tube closure defect often associated with abrogated convergent extension movements and/or defects in the caudal development is spina bifida, which is caused by a closure failure of the neural tube in caudal regions (for review, see Ybot-Gonzalez et al., 2007). *Wnt5a−/−* mice do not usually present spina bifida, although they frequently display a crooked or "wavy" neural tube (black arrow in Fig. 3B), which is associated with PCP defects. Intriguingly, haploinsufficiency for *Lrp6* in a *Wnt5a−/−* background results in spina bifida (unfilled arrow in Fig. 3B) in 50% of *Wnt5a−/−Lrp6+/−* mice, revealing the crucial role of both in neural tube closure.

Anteroposterior defects such as those seen in *Wnt5a−/−Lrp6+/−* embryos could be the result of defective CE or additive defects in truncation of caudal regions. To assess these parameters, we examined the expression of *Uncx4.1*, a marker of the caudal portion of somites, in wild-type, *Wnt5a−/−Lrp6+/+* and *Wnt5a−/−Lrp6+/−* embryos at E9.5. The numbers of somites in littermate mice of these genotypes were not significantly different, but a mild reduction could be observed in *Wnt5a−/−Lrp6+/−* embryos (Fig. 3C). The

distance between somites was greatly decreased in the caudal portion of both *Wnt5a−/−Lrp6+/+* and *Wnt5a−/−Lrp6+/−* embryos (Fig. 3C). These data indicate that the aggravated caudal phenotype in *Wnt5a−/−Lrp6+/−* mice could be a consequence of slight caudal truncation combined with deficient CE.

Wnt5a/Lrp6-Double Deficient Embryos Display Morphogenetic Defects in Presomitic Mesoderm

Wnt5a/Lrp6 mice exhibit a severe phenotype at E10.5 (see Fig. 1A), which is morphologically characterized by severe developmental delay, disrupted caudal development, and defects in heart morphogenesis. These widespread defects led us to speculate that the phenotype is a consequence of earlier defects occurring during gastrulation and early tissue specification. In the early embryo at E8.5, *Wnt5a* is expressed in the posterior part of embryo with high levels in the primitive streak (PS) and presomitic mesoderm (PSM; Yamaguchi et al., 1999a) To analyze the requirement of *Wnt5a* and *Lrp6* in the development of these structures, we investigated the expression of somitogenesis markers and markers of streak-derived mesoderm. In the first set of experiments (Fig. 4A) we performed in situ hybridization for *Hes7,* a marker of the oscillating segmentation clock and *Uncx4.1.* In *Lrp6−/−* embryos, *Hes7* was down-regulated and posterior *Uncx4.1* was weaker or lost. In *Wnt5a−/−* embryos, *Hes7* expression levels were normal, whereas the PS and PSM were shorter in length, and the somites were somewhat compressed but still expressed *Uncx4.1.* In *Wnt5a−/−Lrp6−/−* double mutants, expression of *Hes7* was restored to wild-type levels but the PS instead displayed severe morphogenetic defects. Also *Wnt5a−/−Lrp6−/−* mutants expressed *Uncx4.1* in a striped manner in anterior segmented somites, but appeared fused posteriorly. Finally, the somites of *Wnt5a−/−Lrp6−/−* double mutants were, in some embryos, very compressed compared with their non-*Wnt5a−/−Lrp6−/−* littermates.

To complement this analysis, we looked at the expression of *T* (brachyury), a target gene of Wnt/β-catenin pathway (Yamaguchi et al., 1999b) and a marker of PS/PSM, and *Mesp2*, another Wnt/β-catenin target gene, and marker of presumptive somites in the anterior PSM (Dunty et al., 2008) at E9.0 (Fig. 4B). In *Lrp6−/−* embryos, *T* was expressed in lower levels and *Mesp2* was barely detectable, which confirms that *Lrp6* deficiency causes a Wnt/β-catenin loss-of-function (LOF) in the PSM. In *Wnt5a−/−* embryos, no changes in the expression levels of *T* or *Mesp2* were detected, although the *Mesp2* expression domain had a clearly different shape, which reflects the broader and shorter somites in *Wnt5a−/−* embryos. In *Wnt5a−/−Lrp6−/−* embryos expression of *T* appeared normal and *Mesp2* could be clearly detected. Interestingly, in some embryos, *Mesp2* was present in two stripes, which is reminiscent of β-catenin gain-of-function (GOF) phenotype (Dunty et al., 2008).

In sum, *Hes7* and *T* continued to be expressed strongly in the *Wnt5a−/−Lrp6−/−* double mutants, despite the PSM being shortened, the abnormal morphology of the PS, and the general AP axis shortening. *Lrp6* deficiency resulted in a decrease in PSM markers (*Hes*, *T*), which was not further decreased by loss of *Wnt5a*. In fact, the reverse was seen, and expression of these markers was instead rescued in some double homozygous mice.

Wnt5a/Lrp6-deficient Embryos Exhibit Severe Defects in Neural Tube Development

At E10.5, embryos of all genotypes could still be obtained. While *Wnt5a−/−Lrp6−/−* mice were severely developmentally delayed (Fig. 1), they were still viable and exhibited, for example, a beating heart tube. Gross morphological examination of these embryos indicated that the neural tube was thinner and hollow, compared with littermate controls. We therefore collected sections of neural tube at the level of the forelimb, and stained for actin (with Phalloidin, green in Fig. 5A) and nuclei (with propidium iodide, red) to assess the general morphology of the neural tube.

While *Wnt5a+/+Lrp6−/−* neural tubes were slightly smaller than wild-type littermates, as a consequence of a mild developmental delay, *Wnt5a−/−Lrp6−/−* mice displayed a severely disrupted neural tube of only one- to two-cell layer thickness (Fig. 5A). It is important to note that the *Wnt5a−/−Lrp6−/−* embryo shown here is the most normal *Wnt5a−/−Lrp6−/−* embryo obtained and that others frequently displayed an open neural tube (data not shown) in the caudal region. We asked whether this great reduction in size was in part due to defects in proliferation or differentiation and therefore examined Ki67 (a marker of proliferating cells, green in Fig. 5B) and Tuj1 (a neuronal marker, red). We found that loss of *Lrp6* or *Wnt5a* had negligible effects on the number of proliferating cells (Fig. 5B and data not shown), whereas loss of both *Wnt5a* and *Lrp6* dramatically reduced the number of proliferating cells found in the neural tube at E10.5. Indeed, in some *Wnt5a−/−Lrp6−/−* embryos, no Ki67+ cells could be found (data not shown). The number of Tuj1+ cells was also greatly reduced in *Wnt5a−/−Lrp6−/−* mice (Fig. 5B). Thus, in the absence of *Wnt5a* and *Lrp6*, both proliferation and differentiation of neural tube stem cells is severely impaired.

DISCUSSION

Lrp6 is a co-receptor required for signal transduction in the Wnt/β-catenin pathway (He et al., 2004). After Wnt ligand binding, *Lrp6* is phosphorylated, recruits axin, and in concert with Frizzled receptors and the cytoplasmic protein Dishevelled, blocks the function of the β-catenin destruction complex and promotes β-catenin-dependent transcription. It has been shown that, in most cell types, only some Wnts, for example, Wnt3a, are capable of promoting this signaling pathway, whereas some others, e.g., *Wnt5a*, fail to induce phosphorylation of intracellular parts of Lrp6, and instead activate other signaling pathways, collectively known as noncanonical Wnt signaling pathways (He et al., 2004; Tamai et al., 2004; Bryja et al., 2007a, 2009). This led to the hypothesis that the noncanonical and Wnt/β-catenin pathways are molecularly distinct. As a consequence, *Wnt5a*, a crucial component of the noncanonical pathways, and *Lrp6*, a crucial component of the Wnt/β-catenin pathway should not molecularly interact. This simple view is, however, currently being revised, and it has been suggested that *Lrp6* and *Wnt5a* can functionally interact at several levels.

Evidence in the literature suggest that *Lrp6* and *Wnt5a* could synergize/ antagonize in several ways: (1) *Wnt5a* could act as a β-catenin-activating ligand by means of *Lrp6* (or Lrp5; He et al., 1997; Mikels and Nusse, 2006); (2) *Wnt5a* inhibits Lr_p6-mediated β-catenin activation by means of competition for Dvl, Frizzled, or *Lrp6* itself or by means of other mechanisms (Topol et al., 2003; Westfall et al., 2003; Mikels and Nusse, 2006; Bryja

et al., 2007b, 2009); (3) *Lrp6* could inhibit *Wnt5a*-mediated noncanonical signaling (Tahinci et al., 2007; Bryja et al., 2009); and finally (4) *Lrp6* and *Wnt5a* could control common developmental processes by means of distinct cellular or molecular mechanisms. Multiple modes of interaction between *Lrp6* and *Wnt5a* in development could take place in different cell types, and/or at different time points in the embryo.

Our analyses of *Wnt5a/Lrp6* compound mutants clearly show that *Wnt5a* and *Lrp6* genetically interact. The analyses presented here, however, do not support the first mode of interaction, e.g., *Wnt5a* activates β-catenin signaling by means of *Lrp6.* Several overexpression experiments have shown that specific combinations of Fz receptors and Lrp5 on the cell surface can cause *Wnt5a* to activate β-catenin-dependent transcription both in *Xenopus* embryos and in cultured cells (He et al., 1997; Mikels and Nusse, 2006). We were not able, however, to observe any decrease in the expression of Wnt/β-catenin target genes in Wnt5a-deficient and/or *Wnt5a/Lrp6-deficient* embryos. Specifically, we looked at the posterior part of the developing embryo, where the biological interaction is the most obvious, but neither direct Wnt/β-catenin targets such as *T* (Yamaguchi et al., 1999a) and *Mesp2* (Dunty et al., 2008), nor markers of the oscillating segmentation clock, such as *Hes7,* were negatively affected by loss of *Wnt5a.* These markers are down-regulated in *Lrp6* mutants (this study) and in *Wnt3a* mutants (Dunty et al., 2008), and are completely absent from conditional β-*catenin* LOF mutants (Dunty et al., 2008) This suggests that *Lrp6* acts as a receptor for canonical Wnts in PSM and that *Wnt5a*, which is also present in this region, does not contribute to the activation of β-catenin target genes in the PS-derived mesoderm. Alternatively, *Wnt5a* may primarily antagonize Wnt/b-catenin signaling in the PS/PSM, whereas *Lrp6* functions to prevent *Wnt5a* from doing so by titrating *Wnt5a* away as it was shown to be the case in the noncanonical Wnt signaling (Bryja et al., 2009). In the absence of *Lrp6, Wnt5a* is no longer bound, and antagonizes Wnt/β-catenin signaling (as visualized by the expression of canonical targets such as T, or *Mesp2*) by means of other mechanisms (see below). However, this possibility does not exclude that *Lrp6* acts as the direct positive regulator of Wnt/β-catenin signaling in the PS/PSM. The fact that somites form, visualized by *Uncx4.1* expression, also suggests that the phenotypes observed in *Wnt5a−/−Lrp6−/−* mice are not the result of Wnt/β-catenin LOF.

Our analyses clearly suggest that *Wnt5a* may act, under some circumstances, as an inhibitor of Lrp6-mediated signaling. In most E8.5 embryos, loss of *Wnt5a* rescues down-regulation of *Hes7* and *T* caused by *Lrp6* deficiency. Moreover, in some *Wnt5a/ Lrp6* double-deficient embryos *Mesp2* is present in two stripes, which is a phenotype reminiscent of *β-catenin* GOF in the PS (Dunty et al., 2008). It is also worth noting that *β-catenin* GOF mice fail to turn, similar to *Wnt5a−/−Lrp6−/−* mice. On a molecular level, *Wnt5a* can inhibit Wnt/β-catenin signaling by means of several pathways, including competition for *Lrp6* (Bryja et al., 2009), competition for Dvl (Bryja et al., 2007b), or activation of Ror2-driven signaling (Mikels and Nusse, 2006). Endogenous *Wnt5a* was shown previously to antagonize canonical signaling in vivo, and *Wnt5a* LOF results in Wnt/β-catenin GOF in several developmental processes (Topol et al., 2003; Westfall et al., 2003). We propose that the PSM may represent an additional structure in which endogenous *Wnt5a* reduces Wn^-catenm signaling. However, it remains to be clarified why *Wnt5a* LOF does not have any effect in

Lrp6+/+ mice, and is only observed in an *Lrp6−/−* background when Wnt-β-catenin signaling is reduced.

We and others have recently provided evidence that inhibition of noncanonical *Wnt5a*- or Wnt11-driven signaling by *Lrp6* (or by loss of Dkk1, an *Lrp6* inhibitor) occurs during frog and mouse development (Caneparo et al., 2007; Tahinci et al., 2007; Bryja et al., 2009). We have shown previously that *Lrp6* can bind *Wnt5a* and that *Lrp6*-deficiency results in noncanonical Wnt pathway GOF, which is rescued by depletion of noncanonical Wnt ligands such as *Wnt5a*. Importantly, this only takes place in the tissues where expression of *Wnt5a* is high. In mouse, this mode of interaction is observed in defects in the closure of the neural tube in the midbrain region and during heart outflow tract development (Bryja et al., 2009). Additional phenotypes described here, such as increased compaction of somites and the abnormal shape of PSM in some *Wnt5a−/−Lrp6−/−* embryos, suggest that this mode of interaction can act also in PSM morphogenesis. It is, however, difficult to distinguish this from the alternative possibility; that *Lrp6* acts by means of the Wn^-catenm pathway in somite specification, segmentation clock, and definition of posterior structures, and *Wnt5a* affects convergent extension in this region by means of noncanonical Wnt signaling. Both processes take place in PSM: single *Lrp6* mutants display severe defects in the development of posterior body parts, which is associated with decreased levels of Wn^-catenm target genes (Figs. 2, 4) and *Wnt5a* mutants show clear defects in convergent extension of PSM, which are visualized as higher compaction of somites (*Uncx4.1* staining) and in the formation of somites, which are broader but shorter (*Mesp2* staining). Similar CE-related phenotypes are observed in *Wnt5a*-deficient mice in the inner ear and neural tube (Qian et al., 2007; Andersson et al., 2008).

Interestingly loss of one allele of *Lrp6* has no effect on an otherwise wild-type background (with the exception of low penetrance kinked tail phenotype in adult mice) but induces severe defects in the absence of *Wnt5a.* It is well established that Wn^-catenm signaling is crucial for development of posterior parts of the embryo and is critically required for proper somitogenesis (Yamaguchi, 2001; Dunty et al., 2008). Even partial loss of Wnt^-catenin activity (as demonstrated, for example, by *Lrp6* hypomorph *“ringelschwanz”* mouse) can lead to defects in somitogenesis and posterior development, including spina bifida aperta (Kokubu et al., 2004). Malformations in the most posterior part of tail of *Lrp6+/−* adults, usually as a “kinked” tail, have been observed earlier (Pinson et al., 2000) and also in our experiments (not shown). One can speculate that the loss of *Wnt5a*, which results in a dramatically shortened tail, moves the domain of *Lrp6*-mediated activity more anteriorly to the level of hindlimbs (which is the most posterior part of *Wnt5a*-null embryos), where heterozygosity of *Lrp6* function is sufficient to cause defects such as posterior truncation and associated spina bifida. This phenotype, which was found in *Wnt5a−/−Lrp6+/−* (compared with *Wnt5a−/−* mice), thus probably reflects the combination of highly compacted somites and slightly decreased somite number. Thus, our results indicate that the loss of one allele of *Lrp6* affects posterior development, but only in the context of shorter body axis (*Wnt5a*-deficient bodies), when crucial temporal/spatial coordination of somitogenesis is disturbed because of CE defects.

In summary, we hereby provide evidence that *Lrp6* and *Wnt5a* genetically interact in multiple tissues during mouse development. These interactions, while compatible with multiple mechanisms of interactions, do not support that *Wnt5a* acts as an *Lrp6*-activating ligand in vivo in the tissues examined. Moreover, in addition to the previously described phenotypes showing a crucial role of *Lrp6* as the inhibitor of noncanonical Wnt signaling (Tahinci et al., 2007; Bryja et al., 2009), we hereby demonstrate that *Lrp6* and *Wnt5a* interact to coordinate development of the neural tube, morphogenesis of the PSM, and somitogenesis in mouse.

EXPERIMENTAL PROCEDURES

Animal Maintenance and Embryo Collection

Wnt5a+/− (Yamaguchi et al., 1999a) and *Lrp6+/−* (Pinson et al., 2000) mice were kept on a C57bl6 background, and housed and bred in accordance with the approval of the local ethics committee (Stockholms Norra Djurforsoksetiskanamnd). Noon of day of plug was taken as embryonic day (E) 0.5. Embryos were dissected out in PBS, fixed in 4% paraformaldehyde overnight at 4°C, and then washed in phosphate buffered saline (PBS). Embryos were either dehydrated in a methanol gradient and stored in 100% methanol at −20°C until used in whole-mount in situ hybridization, or transferred to 30% sucrose, rocked overnight, embedded in OCT (Tissue-Tek), and frozen on dry ice for cryostat sectioning and immunohistochemistry. Serial transverse 14-μm sections were collected on SuperFrost glass slides on a cryostat.

Genotyping

DNA extraction and PCR for the *Wnt5a* or *Lrp6* mutant alleles has been described previously (Yamaguchi et al., 1999a; Pinson et al., 2000; Bryja et al., 2009). *SMCX-1* 5′CCGCTGCCAAATTCTTTGG3′ and *SMC4-1* 5′TGAAGCTTTTGGCTTTGAG3′ primers and genotyping of male vs. female, which gives one band in females and two bands of different sizes in males, has been described previously (Agulnik et al., 1997).

In Situ Hybridization

Whole-mount in situ hybridization was performed as previously described (Wilkinson and Nieto, 1993). Embryos were photographed on a stereoscope (Leica, Germany) or and Axiophot compound microscope (Zeiss, Germany). At least three embryos were examined for each probe, and yielded similar results. The following probes were used: *Uncx4.1, Hes7, T*, and *Mesp2* (Dunty et al., 2008).

Immunohistochemistry

Sections/slides were first immersed in PBS for 5 min, and then blocked with 5% goat serum (GS) in phosphate-buffered saline (PBS) with 0.1% Triton-X (PBST) for 1 hr. Primary antibodies were diluted in 5% GS/PBST overnight at 4°C. Slides were then washed in PBS, 3× 15 min, and secondary antibodies, diluted in 5%GS/PBST, were applied for 1 hr at room temperature. The slides were then washed again, 3× 15 min, counterstained with Topro-3 (Invitrogen) or propidium iodide (Invitrogen) and washed twice more. Slides were mounted in glycerol/PBS 9:1.

The following antibodies were used: rabbit anti-Ki67 (1:800, Abcam), mouse anti-Tuj1 (βIII tubulin, 1:1,000, BD Biosciences), Alexa488 anti-mouse and Alexa555 anti-rabbit (1:1,000, Molecular Probes). Phalloidin (Invitrogen) staining was carried out according to the manufacturer's instructions.

All images were acquired on a Zeiss LSM 510 (Zeiss, Germany), with Zeiss software.

ACKNOWLEDGMENTS

We thank Johnny Söderlund and Alessandra Nanni for technical and secretarial assistance, respectively, as well as Susanne Ahnstrand and Cecilia Olsson of the MBB animal house facility, for excellent animal care. We also thank William Skarnes (Sanger Institute, Cambridge) for providing *Lrp6*-deficient mice. V.B. was funded by an EMBO Installation Grant and the Ministry of Education Youth and Sports of the Czech Republic. E.A. was funded by the Swedish Foundation for Strategic Research (INGVAR and CEDB), Swedish Research Council (VR2008:2811 and DBRM), Norwegian Research Council, Karolinska Institutet, Michael J. Fox Foundation, and European Commission (Eurostemcell). The authors declare no conflict of interest.

Grant sponsor: EMBO; Ministry of Education Youth and Sports of the Czech Republic; Grant number: MSM 0021622430; Grant sponsor: Swedish Foundation for Strategic Research (INGVAR and CEDB); Swedish Research Council; Grant number: VR2008:2811 and DBRM; Grant sponsor: Norwegian Research Council; Grant sponsor: Karolinska Institutet; Grant sponsor: Michael J. Fox Foundation; Grant sponsor: European Commission (Eurostemcell).

REFERENCES

Adamska M, Billi AC, Cheek S, Meisler MH. 2005 Genetic interaction between Wnt7a and *Lrp6* during patterning of dorsal and posterior structures of the mouse limb. Dev Dyn 233:368–372. [PubMed: 15880584]

Agulnik AI, Bishop CE, Lerner JL, Agulnik SI, Solovyev VV. 1997 Analysis of mutation rates in the SMCY/SMCX genes shows that mammalian evolution is male driven. Mamm Genome 8:134–138. [PubMed: 9060413]

Andersson ER, Prakash N, Cajanek L, Minina E, Bryja V, Bryjova L, Yamaguchi TP, Hall AC, Wurst W, Arenas E. 2008 Wnt5a regulates ventral midbrain morphogenesis and the development of A9-A10 dopaminergic cells in vivo. PLoS ONE 3:e3517. [PubMed: 18953410]

Bilic J, Huang YL, Davidson G, Zimmermann T, Cruciat CM, Bienz M, Niehrs C. 2007 Wnt induces LRP6 signalosomes and promotes dishevelled-dependent LRP6 phosphorylation. Science 316:1619–1622. [PubMed: 17569865]

Bryja V, Gradl D, Schambony A, Arenas E, Schulte G. 2007a beta-arrestin is a necessary component of Wnt/beta-catenin signaling in vitro and in vivo. Proc Natl Acad Sci USA 104:6690–6695. [PubMed: 17426148]

Bryja V, Schulte G, Rawal N, Grahn A, Arenas E. 2007b Wnt-5a induces Dishevelled phosphorylation and dopaminergic differentiation via a CK1-dependent mechanism. J Cell Sci 120:586–595. [PubMed: 17244647]

Bryja V, Andersson ER, Schambony A, Esner M, Bryjova L, Biris KK, Hall AC, Kraft B, Cajanek L, Yamaguchi TP, Buckingham M, Arenas E. 2009 The extracellular domain of Lrp5/6 inhibits noncanonical Wnt signaling in vivo. Mol Biol Cell 20:924–936. [PubMed: 19056682]

Caneparo L, Huang YL, Staudt N, Tada M, Ahrendt R, Kazanskaya O, Niehrs C, Houart C. 2007 Dickkopf-1 regulates gastrulation movements by coordinated modulation of Wnt/beta catenin and Wnt/PCP activities, through interaction with the Dally-like homolog Knypek. Genes Dev 21:465–480. [PubMed: 17322405]

Castelo-Branco G, Andersson ER, Minina E, Sousa KM, Ribeiro D, Kokubu C, Imai K, Prakash N, Wurst W, Arenas E. 2009 Delayed dopaminergic neuron differentiation in *Lrp6* mutant mice. Dev Dyn 238:000–000.

Dunty WC Jr, Biris KK, Chalamalasetty RB, Taketo MM, Lewandoski M, Yamaguchi TP. 2008 Wnt3a/beta-catenin signaling controls posterior body development by coordinating mesoderm formation and segmentation. Development 135:85–94. [PubMed: 18045842]

Hamblet NS, Lijam N, Ruiz-Lozano P, Wang J, Yang Y, Luo Z, Mei L, Chien KR, Sussman DJ, Wynshaw-Boris A. 2002 Dishevelled 2 is essential for cardiac outflow tract development, somite segmentation and neural tube closure. Development 129:5827–5838. [PubMed: 12421720]

He X, Saint-Jeannet JP, Wang Y, Nathans J, Dawid I, Varmus H. 1997 A member of the Frizzled protein family mediating axis induction by Wnt-5A. Science 275: 1652–1654. [PubMed: 9054360]

He X, Semenov M, Tamai K, Zeng X. 2004 LDL receptor-related proteins 5 and 6 in Wnt/beta-catenin signaling: arrows point the way. Development 131:1663–1677. [PubMed: 15084453]

Kokubu C, Heinzmann U, Kokubu T, Sakai N, Kubota T, Kawai M, Wahl MB, Galceran J, Grosschedl R, Ozono K, Imai K. 2004 Skeletal defects in ringelschwanz mutant mice reveal that Lrp6 is required for proper somitogenesis and osteogenesis. Development 131: 5469–5480. [PubMed: 15469977]

Logan CY, Nusse R. 2004 The wnt signaling pathway in development and disease. Annu Rev Cell Dev Biol 20:781–810. [PubMed: 15473860]

Mikels AJ, Nusse R. 2006 Purified Wnt5a protein activates or inhibits beta-catenin-TCF signaling depending on receptor context. PLoS Biol 4:e115. [PubMed: 16602827]

Montcouquiol M, Crenshaw EB III, Kelley MW. 2006 Noncanonical Wnt signaling and neural polarity. Annu Rev Neurosci 29:363–386. [PubMed: 16776590]

Moon RT, Campbell RM, Christian JL, McGrew LL, Shih J, Fraser S. 1993 Xwnt-5A: a maternal Wnt that affects morphogenetic movements after overexpression in embryos of Xenopus laevis. Development 119:97–111. [PubMed: 8275867]

Pinson KI, Brennan J, Monkley S, Avery BJ, Skarnes WC. 2000 An LDL-receptor-related protein mediates Wnt signalling in mice. Nature 407: 535–538. [PubMed: 11029008]

Qian D, Jones C, Rzadzinska A, Mark S, Zhang X, Steel KP, Dai X, Chen P. 2007 Wnt5a functions in planar cell polarity regulation in mice. Dev Biol 306:121–133. [PubMed: 17433286]

Schleiffarth JR, Person AD, Martinsen BJ, Sukovich DJ, Neumann A, Baker CV, Lohr JL, Cornfield DN, Ekker SC, Petryk A. 2007 Wnt5a is required for cardiac outflow tract septation in mice. Pediatr Res 61:386–391. [PubMed: 17515859]

Schulte G, Bryja V, Rawal N, Castelo-Branco G, Sousa KM, Arenas E. 2005 Purified Wnt-5a increases differentiation of midbrain dopaminergic cells and dishevelled phosphorylation. J Neurochem 92:1550–1553. [PubMed: 15748172]

Sokol S, Christian JL, Moon RT, Melton DA. 1991 Injected Wnt RNA induces a complete body axis in Xenopus embryos. Cell 67:741–752. [PubMed: 1834344]

Tahinci E, Thorne CA, Franklin JL, Salic A, Christian KM, Lee LA, Coffey RJ, Lee E. 2007 Lrp6 is required for convergent extension during Xenopus gastrulation. Development 134:4095–4106. [PubMed: 17965054]

Tamai K, Zeng X, Liu C, Zhang X, Harada Y, Chang Z, He X. 2004 A mechanism for Wnt coreceptor activation. Mol Cell 13:149–156. [PubMed: 14731402]

Topol L, Jiang X, Choi H, Garrett-Beal L, Carolan PJ, Yang Y. 2003 Wnt-5a inhibits the canonical Wnt pathway by promoting GSK-3-independent beta-catenin degradation. J Cell Biol 162:899–908. [PubMed: 12952940]

Torres MA, Yang-Snyder JA, Purcell SM, DeMarais AA, McGrew LL, Moon RT. 1996 Activities of the Wnt-1 class of secreted signaling factors are antagonized by the Wnt-5A class and by a dominant negative cadherin in early Xenopus development. J Cell Biol 133:1123–1137. [PubMed: 8655584]

Vainio S, Heikkila M, Kispert A, Chin N, McMahon AP. 1999 Female development in mammals is regulated by Wnt-4 signalling. Nature 397:405–409. [PubMed: 9989404]

Westfall TA, Brimeyer R, Twedt J, Gladon J, Olberding A, Furutani-Seiki M, Slusarski DC. 2003 Wnt-5/pipetail functions in vertebrate axis formation as a negative regulator of Wnt/beta-catenin activity. J Cell Biol 162:889–898. [PubMed: 12952939]

Wilkinson DG, Nieto MA. 1993 Detection of messenger RNA by in situ hybridization to tissue sections and whole mounts. Methods Enzymol 225:361–373. [PubMed: 8231863]

Wong GT, Gavin BJ, McMahon AP. 1994 Differential transformation of mammary epithelial cells by Wnt genes. Mol Cell Biol 14:6278–6286. [PubMed: 8065359]

Yamaguchi TP. 2001 Heads or tails: Wnts and anterior-posterior patterning. Curr Biol 11:R713–724. [PubMed: 11553348]

Yamaguchi TP, Bradley A, McMahon AP, Jones S. 1999a A Wnt5a pathway underlies outgrowth of multiple structures in the vertebrate embryo. Development 126:1211–1223. [PubMed: 10021340]

Yamaguchi TP, Takada S, Yoshikawa Y, Wu N, McMahon AP. 1999b T (Brachyury) is a direct target of Wnt3a during paraxial mesoderm specification. Genes Dev 13:3185–3190. [PubMed: 10617567]

Yang DH, Yoon JY, Lee SH, Bryja V, Andersson ER, Arenas E, Kwon YG, Choi KY. 2009 Wnt5a is required for endothelial differentiation of embryonic stem cells and vascularization via pathways involving both Wnt/beta-catenin and protein kinase Calpha. Circ Res 104:372–379. [PubMed: 19096028]

Ybot-Gonzalez P, Savery D, Gerrelli D, Signore M, Mitchell CE, Faux CH, Greene ND, Copp AJ. 2007 Convergent extension, planar-cell-polarity signalling and initiation of mouse neural tube closure. Development 134:789–799. [PubMed: 17229766]

Zhou CJ, Molotkov A, Song L, Li Y, Pleasure DE, Pleasure SJ, Wang YZ. 2008 Ocular coloboma and dorsoventral neuroretinal patterning defects in Lrp6 mutant eyes. Dev Dyn 237:3681–3689. [PubMed: 18985738]

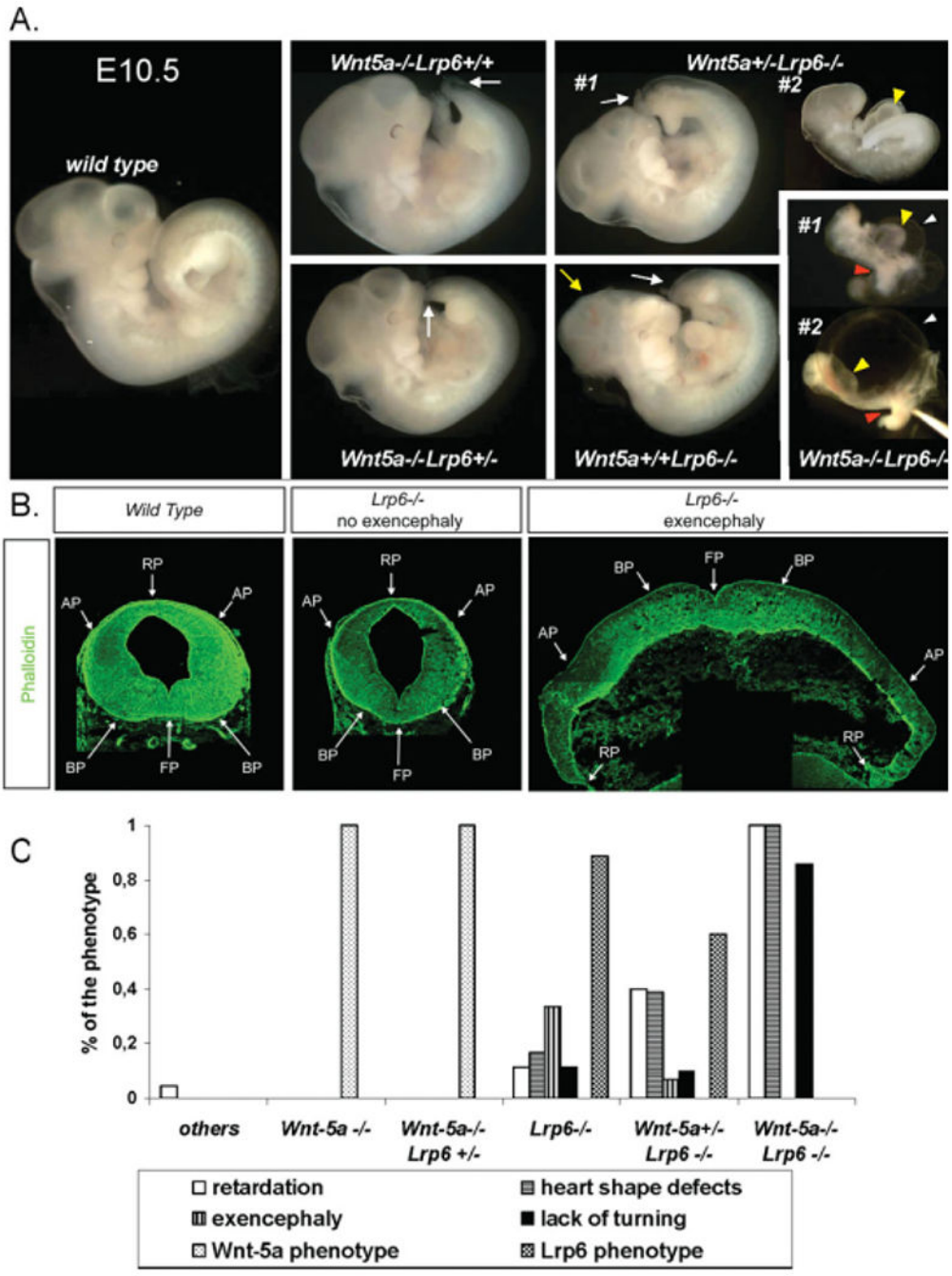

Fig. 1.

General developmental phenotypes of *Wnt5a* and *Lrp6* single and double mutant mice at E10.5. **A:** General morphology of *Wnt5a/Lrp6* compound mutants at E10.5. Arrows indicate the shortened tail in *Wnt5a−/−Lrp6+/+* embryo and kinked tail and exencephaly in a *Lrp6−/−* embryo. Two specimens of *Wnt5a+/−Lrp6−/−* and *Wnt5a−/−Lrp6−/−* embryos are shown to demonstrate the variability of the phenotype. Yellow arrowheads indicate defective heart tube, white arrowheads indicate enlarged pericardium, and red arrowheads indicate defects in embryo turning. **B:** Normal and exencephalic midbrains of embryonic day (E) 12.5 wild-

type (WT) and *Lrp6−/−* embryos were sectioned and stained with phalloidin to visualize morphogenetic changes, including exencephaly in the midbrain region. **C:** Quantification of the observed phenotype is based on 4 *Wnt5a−/−*, 12 *Wnt5a−/−Lrp6+/−*, 9 *Lrp6−/−*, 30 *Wnt5a+/−Lrp6−/−*, and 7 *Wnt5a−/−Lrp6−/−* embryos at E10.5. See text for details.

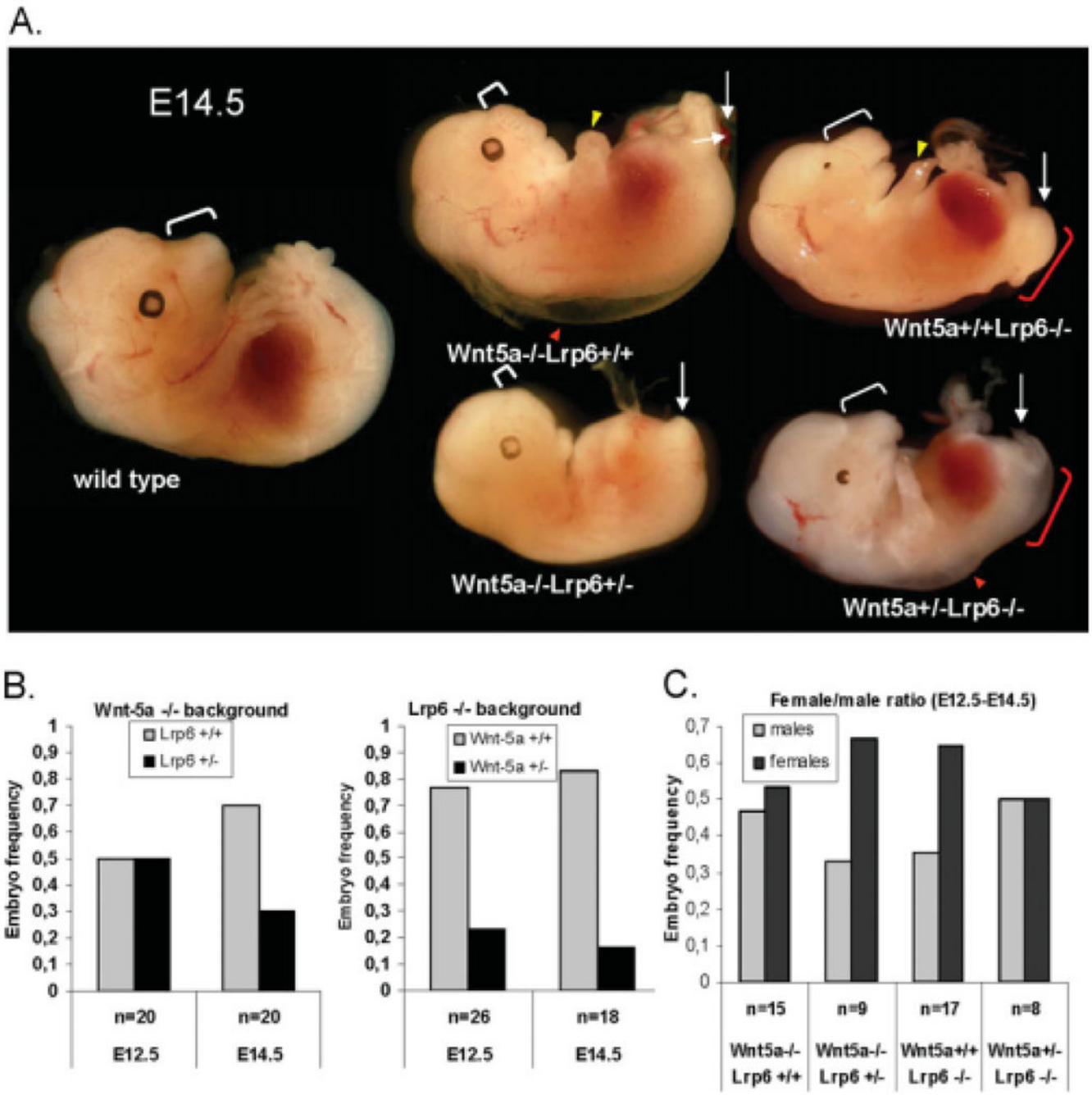

Fig. 2.

Impact of loss of *Wnt5a* or *Lrp6* on phenotype at embryonic day (E) 14.5, survival and gender selection. **A:** General morphology of Wnt5a/Lrp6 compound mutants at E14.5. Yellow arrowheads indicate limb deformities, red arrowheads indicate edema, and white arrows indicate defects in the posterior development. White brackets indicate snout length and shortening in *Wnt5a−/−* embryos, and red bracket indicates spina bifida. **B:** Survival analysis of *Wnt5a−/−Lrp6+/+* and *Wnt5a−/−Lrp6+/−* embryos (first graph), and *Wnt5a+/+Lrp6−/−*, and *Wnt5a+/−Lrp6−/−* embryos (second graph) at E12.5 and E14.5. Graphs

indicate proportion of embryos with the indicated genotype within all *Wnt5a−/−* or *Lrp6−/−* embryos. n indicates number of embryos in the set. **C:** Analysis of female/male ratio as indicated by polymerase chain reaction (PCR) of embryos between E12.5 and E14.5. n indicates number of embryos in the set.

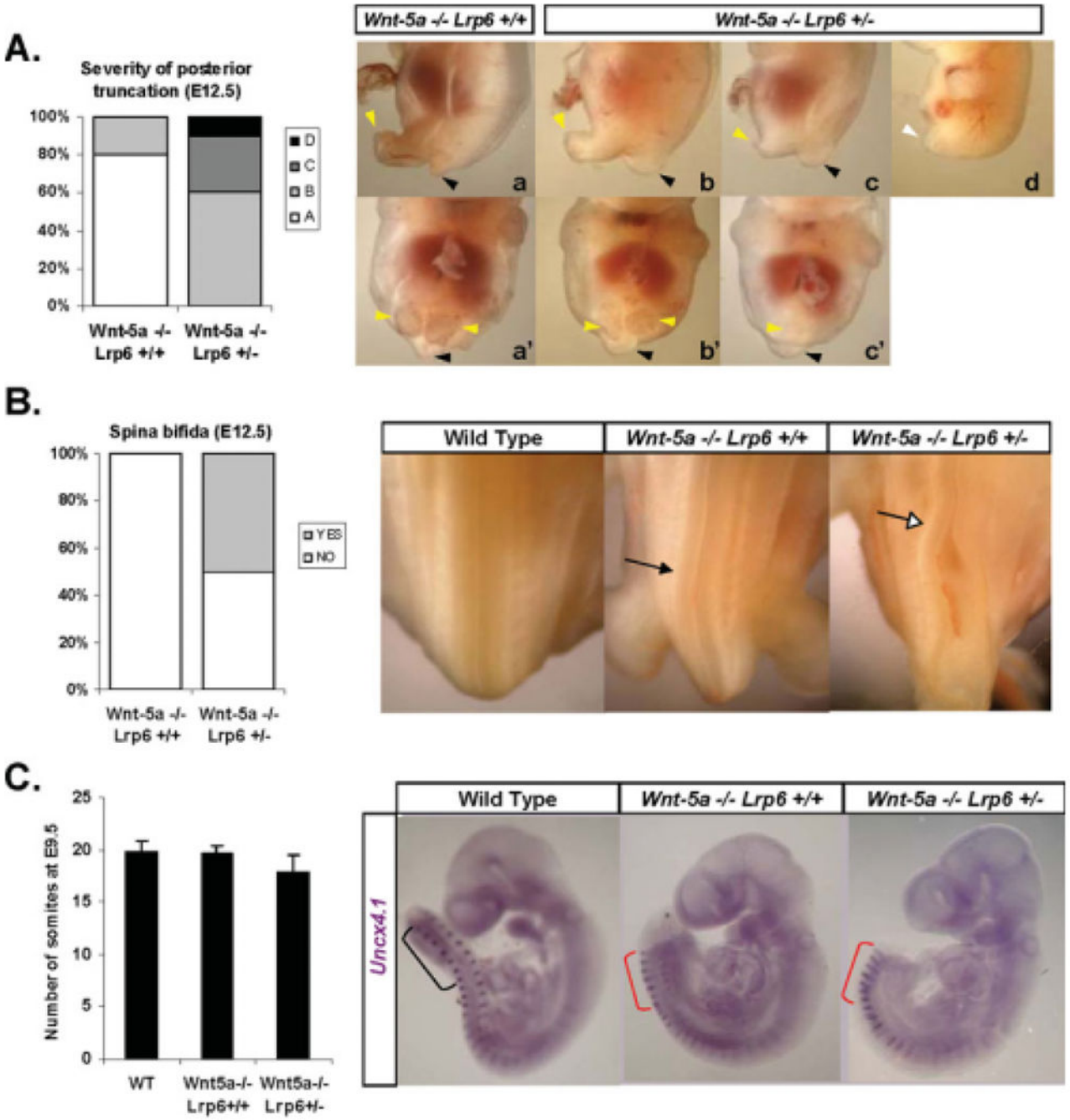

Fig. 3.

Ablation of Lrp6 on a *Wnt5a−/−* background aggravates caudal developmental defects. **A:** *Wnt5a−/−Lrp6+/+* and *Wnt5a−/−Lrp6+/−* embryos were classified based on the severity of their posterior phenotype into four groups (A,B,C,D). Typical characteristics of these groups are depicted in subpanels a–d (lateral view) and a′–c′ (ventral view), and described in the text. Yellow arrowheads indicate residual hindlimbs, black arrowheads indicate tail rudiments. Analysis of 10 *Wnt5a−/−Lrp6+/+* and 10 *Wnt5a−/−Lrp6+/−* demonstrates that the level of posterior truncation is more severe in *Wnt5a−/−Lrp6+/−*. **B:** The same set of

embryos as in A was analyzed for presence of spina bifida (indicated by open arrow). Black arrow indicates nonstraight neural tube seen in *Wnt5a−/−* mice. *Wnt5a−/−Lrp6+/−* but not *Wnt5a−/−Lrp6+/+* embryos frequently display spina bifida. **C:** Wild-type, *Wnt5a−/−Lrp6+/+*, and *Wnt5a−/−Lrp6+/−* embryos were collected at embryonic day (E) 9.5 and stained for *Uncx4.1* to visualize somites. Somites were counted in each embryo, and the results (mean+SE) are shown in the graph. Embryos with *Wnt5a−/−* background show more compacted somites (red brackets).

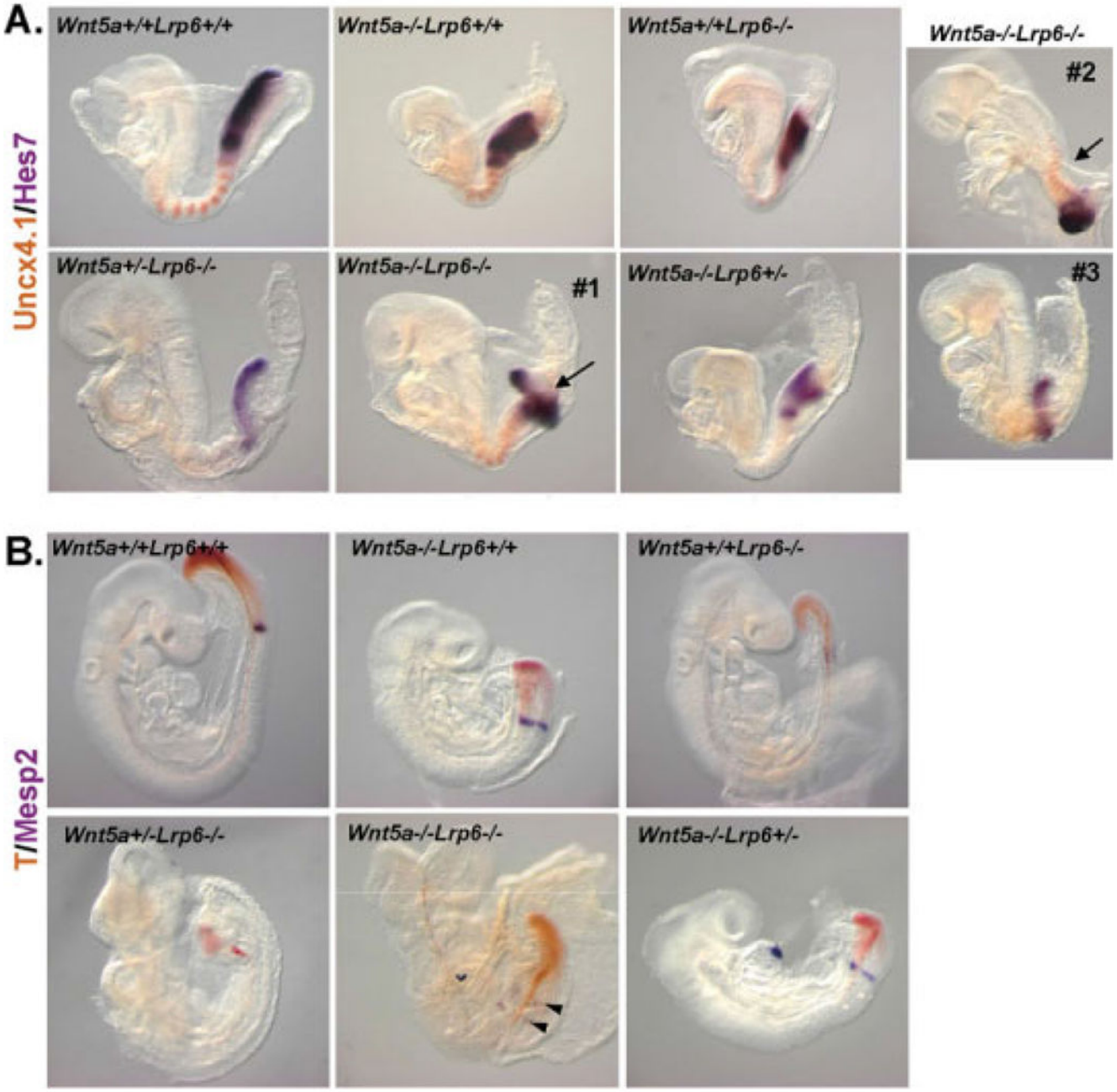

Fig. 4.

Defects in presomitic mesoderm in *Wnt5a* and *Lrp6* compound mutants. **A:** Embryos with indicated genotypes were stained at embryonic day (E) 8.5 for *Uncx4.1* (brown) and Hes7 (purple) using whole-mount in situ hybridization. Three different *Wnt5a−/−Lrp6−/−* embryos are shown. Defects in the morphogenesis of presomitic mesoderm are indicated by arrows. **B:** Embryos between embryonic day (E) 8.75–E9.0 were stained for T (brachyury; brown) and Mesp2 (purple). Abnormal expression of Mesp2 in *Wnt5a−/−Lrp6−/−* is indicated by arrowheads.

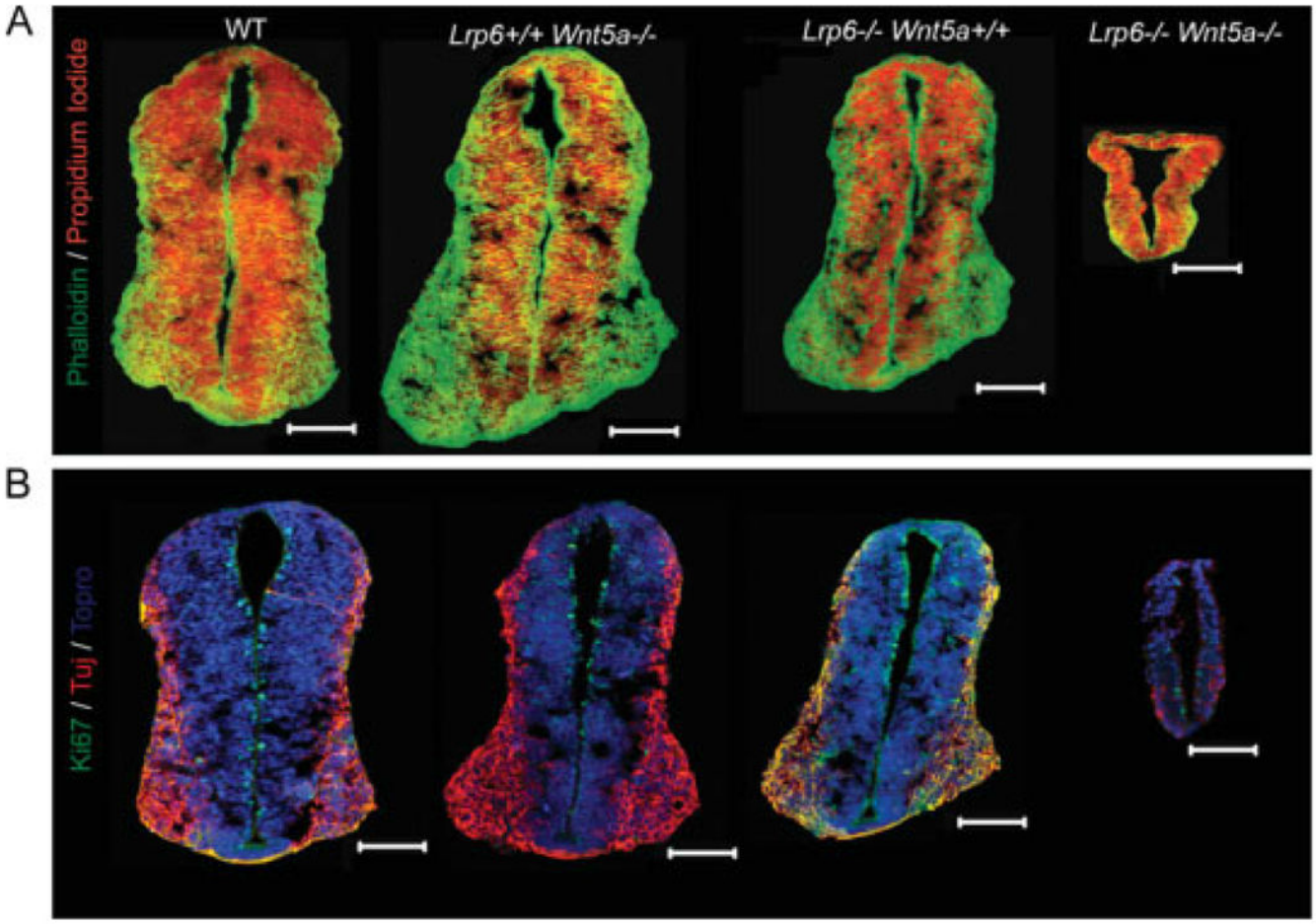

Fig. 5.

Decreased proliferation and neuron number in *Wnt5a−/−Lrp6−/−* mice. Neural tubes of mouse embryos with the indicated genotypes were sectioned at embryonic day (E) 10.5. **A,B:** Cross-sections of neural tube stained either for actin (A; phalloidin; green) and cell nuclei (propidium iodide, red), or for proliferation marker Ki67 (B; green), neuronal marker TuJ (red), and cell nuclei (Topro, blue). Scale bar = 100 μm.